rRNA Chemical Groups Required for Aminoglycoside Binding†

Scott C. Blanchard, Dominique Fourmy, Robert G. Eason, and Joseph D. Puglisi*

Department of Structural Biology, Stanford University School of Medicine Fairchild Center D105A Stanford, California 94305-5400

Received December 19, 1997; Revised Manuscript Received March 31, 1998

ABSTRACT: Through an affinity chromatography based modification-interference assay, we have identified chemical groups within *Escherichia coli* 16S ribosomal RNA sequence that are required for binding the aminoglycoside antibiotic paromomycin. Paromomycin was covalently linked to solid support via a nine atom spacer from the 6‴-amine of ring IV, and chemical modifications to an A-site oligonucleotide that disrupted binding were identified. Positions in the RNA oligonucleotide that correspond to G1405(N7), G1491(N7), G1494(N7), A1408(N7), A1493(N7), A1408(N1), A1492(N1), and A1493(N1), as well as the pro-*R* phosphate oxygens of A1492 and A1493 in 16S rRNA are chemical groups that are essential for a high-affinity RNA−paromomycin interaction. These data are consistent with genetic, biochemical, and structural studies related to neomycin-class antibiotics and provide additional information for establishing an exact model for their interaction with the ribosome.

Aminoglycoside antibiotics are powerful inhibitors of prokaryotic cell growth that interact directly with ribosomal RNA (rRNA) (*1*) (Figure 1a). Aminoglycosides interact with nucleotides in the 30S ribosomal subunit A-site, where the codon−anticodon interaction occurs (*1*), promoting improper choice of aminoacyl-tRNA during elongation and inhibiting translocation of the tRNA−mRNA complex from the A-site to the P-site (*2*, *3*). The neomycin subclass of aminoglycosides, which includes paromomycin (Figure 1c), do not compete with aminoacyl-tRNA binding to ribosomes at the A-site; instead, they decrease the dissociation rate of A-site bound aminoacyl-tRNAs (*4*). Thus, aminoglycosides bind to a site in rRNA that is in close proximity to the codon−anticodon-binding site and alter kinetic steps essential for proper tRNA selection and efficient translocation.

RNA oligonucleotides reconstitute the aminoglycoside-binding site of the ribosome (*5*−*7*). A 27 nucleotide RNA (A-site RNA) binds aminoglycoside antibiotics with similar affinity and specificity as 30S subunits (*5*) (Figure 1b). Nucleotides that are required for aminoglycoside binding to the oligonucleotide have been identified by mutagenesis and quantitative footprinting; essential nucleotides for high-affinity binding are clustered around the highly conserved asymmetric loop of the A-site.

The solution structure of the paromomycin−RNA oligonucleotide complex revealed important details of the RNA−antibiotic interaction (*8*). Paromomycin binds in the major groove of the RNA, in a binding pocket formed by an A−A base pair and a bulged adenosine. The antibiotic packs tightly against the RNA and makes specific contacts to nucleotides previously shown to be important for paromomycin binding in vivo and in vitro (*5*, *9*). A1408 of the A−A base-pair is conserved in all prokaryotic species, whereas its base pairing partner, A1493, and the bulged nucleotide, A1492, are universally conserved. Both A1492-(N1) and A1493(N1) are footprinted by A-site tRNA and mRNA codon on the ribosome (*10*).

Structural comparison of the free and bound forms of A-site RNA demonstrated that antibiotic binding induces a local conformational change in the RNA centered around the A−A base pair (*11*). In the RNA−drug complex, A1408, A1492, and A1493 have reduced conformational dynamics and are shifted toward the minor groove by more than 2 Å; this displacement induces a kink in the backbone at the A1493 phosphate.

To examine the specific contribution of RNA−paromomycin and RNA−RNA contacts to the RNA−drug interaction, we have designed a chemical modification-interference assay to probe the paromomycin-binding site. Our assay, based on affinity chromatography using sepharose 4B matrix derivatized with paromomycin, enabled us to determine the chemical groups in A-site RNA that are required for aminoglycoside binding. A distinct spatial organization of phosphates and other hydrogen-bonding groups in the paromomycin-binding site were identified that contribute to high-affinity binding. These data are in excellent agreement with proposed contacts in the RNA−paromomycin structure. Specific interaction of the tethered aminoglycoside with the A-site RNA suggests that derivatization of neomycin class antibiotics is possible and that such derivatives are useful tools to study aminoglycoside function.

MATERIALS AND METHODS

Designing the A-Site RNA Oligonucleotide. Aminoglycosides bind to the *Escherichia coli* 30S subunit in a region of 16S rRNA defined by nucleotides 1404−1412 and 1488−1497; this region constitutes the core of the highly conserved

† Supported by grants from NIH (R01-GM51266-01A1), Packard Foundation, and Lucille Markey Charitable Trust. Dominique Fourmy was supported by a grant from INSERM (Institute Nationale de la Santé et de la Recherche Medicale).

* To whom all correspondence should be addressed. E-mail: puglisi@stanford.edu. Phone: (650) 498-4397. Fax: (650) 723-8464.

S0006-2960(97)03125-5 CCC: $15.00
Published on Web 05/07/1998

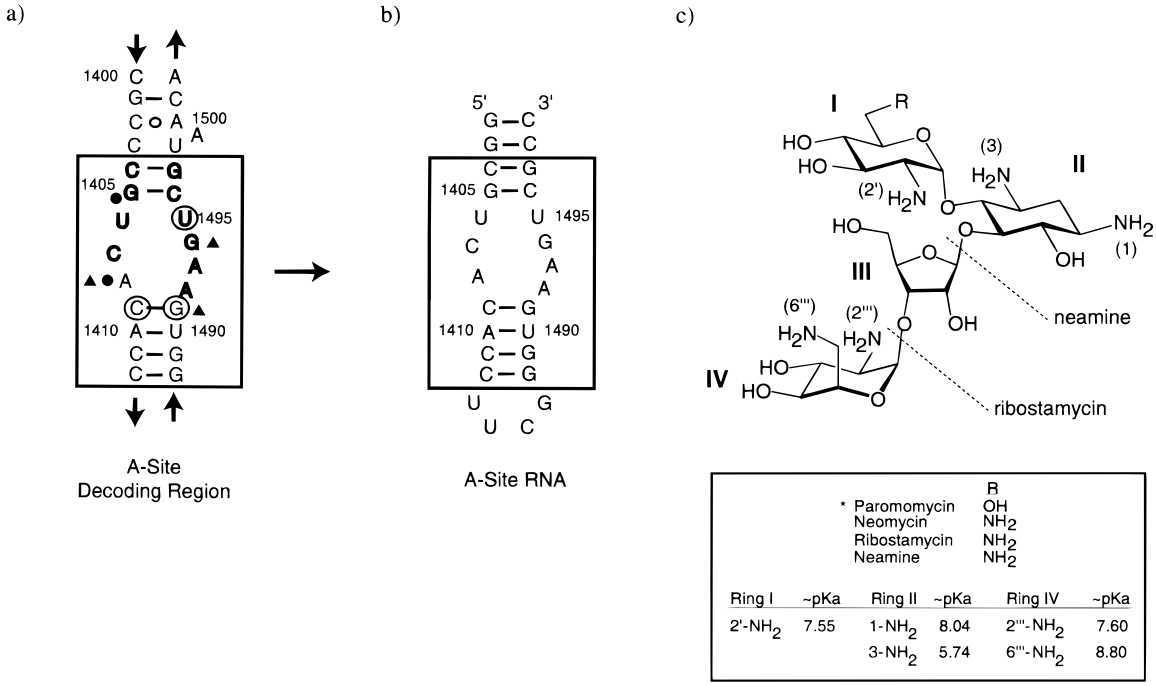

FIGURE 1: (a) The A-site of the 30S subunit (boxed) is localized to the 3′ domain of 16S ribosomal RNA. Shown is the nucleotide sequence and the secondary structure in this region of the ribosome. (▲) Nucleotides in rRNA that are protected from modification by chemical probes upon addition of aminoglycoside antibiotics. (●) Nucleotides that are modified in aminoglycoside resistant organisms. Nucleotides that are <95% conserved in all organisms and subcellular organelles are highlighted in bold script. Circled nucleotides are those whose identity has been genetically linked to aminoglycoside resistance (see text). (b) This small RNA, designated as A-site RNA, mimics rRNA structure in the A-site and recapitulates the aminoglycoside binding properties of the 30S rRNA subunit (*5*, *8*). (c) Covalent structures of the neomycin-class aminoglycoside antibiotics are illustrated. Neamine is equivalent to neomycin but it lacks rings III and IV whereas ribostamycin differs from neomycin in that it lacks just ring IV. Rings I and II are conserved elements of all aminoglycosides that target the A-site of rRNA. The boxed information indicates the chemical substitution pattern for the individual neomycin-class aminoglycosides and includes the estimated pK_as of each numbered amine functionality as determined for neomycin by NMR (*29*) (see Discussion).

A-site (*1*, *10*). Aminoglycoside binding to the 30S subunit alters the accessibility of rRNA in the A-site and the 530 loop to chemical probes, but evidence suggests that aminoglycoside effects on the 530 loop are indirect (*12*). Consistent with this model, mutations or modifications in rRNA that disrupt aminoglycoside binding occur within the 1404−1412 and 1488−1497 A-site rRNA sequence but have not been observed in the 530 loop region. The model oligonucleotide used in this study contains nucleotides 1404−1412 and 1488−1497 of the *E. coli* 16S rRNA sequence; this RNA recapitulates the aminoglycoside binding properties of the ribosome by mimicking the RNA structure of the A-site (*5*, *8*, *13*). To ensure stable, monomeric structure in solution, two G−C base pairs and a 5′-UUCG-3′ tetraloop flank the isolated A-site rRNA sequence (Figure 1b).

Preparing an Affinity Column for the Modification Interference Assay. The free base form of paromomycin sulfate (Sigma) was prepared by desalting the compound over TSK−Gel Toyopearl DEAE−650 M (Supelco) prewashed with 1 M NaOH and equilibrated to pH = 7.0 with water. Sepharose 4B matrix activated with 6-aminohexanoic acid *N*-hydroxysuccinimide ester (Sigma) was washed with 50 mL of ice-cold 1 mM HCl before coupling to paromomycin. Paromomycin-free base was covalently linked to the activated matrix by vortexing 0.5 g of the washed matrix with 0.025 μmol of paromomycin free base at room temperature for 1 h in 2 mL of 100 mM $NaHCO_3$ and 500 mM NaCl at pH = 6.0, 8.0, or 10.0. The stoichiometry of the coupling reaction was chosen to ensure that the column matrix was not derivatized to greater than 25 nmol of paromomycin/mL of column resin. Residual NHS-ester activated matrix was capped by placing the slurry of resin into a 10 mL Bio-spin column (Bio-Rad) and washing with 25 mL of 100 mM Tris-HCl pH = 8.0 at room temperature.

Preparing RNAs for the Modification Interference Assay. DNA oligonucleotides for use as in vitro transcription templates were synthesized by standard phosphoramidite chemistry (Millipore) and purified by either 20 or 10% 19:1 acrylamide:bisacrylamide denaturing (7 M urea) gel electrophoresis. RNA molecules were synthesized by in vitro transcription with T7 RNA polymerase (*14*). Transcribed RNAs were purified by 20% 19:1 acrylamide:bisacrylamide denaturing gel electrophoresis (7 M urea) and electroeluted (Schleicher and Schuell). RNA (30 pmol) was 3′ end-labeled using cytidine 5′,3′-bisphosphate (Amersham) and T4 RNA ligase (New England Biolabs) and electrophoretically purified under denaturing conditions. End-labeled RNA was passively eluted from the gel at 4 °C using 100 mM NH_4OAc, pH = 7.0, ethanol precipitated, 0.2 μm microfuge filtered (Lida), and dialyzed for 14 h against water using a microdialysis apparatus (Life Tech).

RNA (in 10 mM NaH_2PO_4 buffer, pH = 7.0) was modified using dimethyl sulfate (DMS) or diethyl pyrocarbonate (DEPC) (Aldrich) under thermally denaturing conditions (85 °C) to statistically modify 20% of the RNA pool. RNA with phosphorothioate modifications was synthesized by in vitro transcription in four separate reactions (corresponding to A, U, C, and G). In vitro transcription reactions, labeling and

purifications were performed exactly as described above except that the reaction conditions were for transcription changed to be 2 mM in three of the NTPs and 1 mM in the NTP to be modified, and the reactions were doped with 1 part NTPαS to *X* parts of the same normal NTP (where *X* is the total number of that nucleotide in the RNA sequence); this corresponds to 250 μM ATPαS, 200 μM UTPαS, 111.25 μM CTPαS, and 111.25 μM GTPαS (*15*). Each reaction generated a population of RNAs containing a collection of single phosphorothioate linkages.

Assay Conditions and Sample Analysis. All modification-interference experiments were performed in gravity-fed (~1 mL/min) 150 mM NH_4OAc and 10 mM Na_2PO_4, pH = 7.0 at 4 °C. The paromomycin-Sepharose 4B column was preequilibrated with 50 vol of running buffer before each experiment. Approximately 8 pmol of 3′ end-labeled, modified RNA, (~2.5×10^5 cpm) was loaded into 1 mL of running buffer void volume above the column matrix to begin each experiment. The RNA was allowed to load onto the column at ~1 mL/min and the same flow rate was used to wash the matrix with 35 column vol of running buffer to elute weakly bound RNA. RNA that remained bound after this step was eluted with 1 M NH_4OAc, pH = 7.0. Both flow-through and salt-eluted RNA samples were collected in 1 mL fractions in screw-top Eppendorf tubes. Samples were immediately frozen with liquid nitrogen and Cerenkov counted. Samples were subsequently lyophilized to dryness, resuspended in water, ethanol precipitated, and dialyzed 12 h against 1 L of water using a microdialysis apparatus. Dialyzed fractions were then ethanol precipitated, 70% ethanol washed, and lyophilized to dryness to adjust sample volumes. Cleavage at modified positions was induced by published procedures for each type of modification (*16*−*18*) and detected by denaturing gel electrophoresis and subsequent autoradiography. Experimental results were quantified using a Molecular Dynamics phosphorimager.

Characterizing the Paromomycin Linkage to Solid Support: *Mock Coupling of Paromomycin to 6-(2,4-Dinitrophenyl)Aminohexanoic Acid*. Paromomycin-free base (8.6 mg) was coupled to 5 mg of 6-(2,4-dinitrophenyl)aminohexanoic acid succinimidyl ester (DNP−NHSE) (14 mM each), in 1 mL of 100 mM $NaHCO_3$, pH = 10.0, and 500 mM NaCl by vortexing for 1 h at room temperature. The reaction mixture was then diluted into 10 mL of acetonitrile and 0.1% trifluoroacetic acid to stop the reaction. This solution was diluted further to 50% methanol and analyzed at 360 nm (an absorbance maximum for the dye) by reverse phase HPLC (Rainin). This reaction mixture (20 μL) was injected onto a 5 μm, 4.6 mm × 25 cm Dynamax C18 column (Rainin) equilibrated to 0.1% aqueous trifluoroacetic acid. The reaction products were eluted with a gradient from 0 to 60% 0.1% trifluoroacetic acid in acetonitrile over 25 min. Under these conditions DNP−paromomycin-linked products could be separated from the starting material to assess reaction completion and the elution times of the reaction products.

DNP−paromomycin product (0.5 mg) was prepared by scaling up the procedure and isolating the major reaction product by HPLC. The isolated material was lyophilized to dryness and resuspended in either 300 μL of D_2O or H_2O/D_2O (9/1) and 10 mM sodium phosphate at pH = 7.0. The sample concentration was ~10 mM. Standard NOESY, DQF−COSY, and TOCSY data were acquired. NOESY experiments were conducted with mixing times of 50 and 200 ms. TOCSY experiments were acquired with mixing times of 15 and 70 ms. All NMR experiments were performed at 25 °C on a Varian Unity+ 500 MHz spectrometer, and data were processed using Varian software.

RESULTS

Preparation of Aminoglycoside Affinity Columns. Preparing affinity columns using paromomycin or other aminoglycosides is difficult given that these compounds possess many nucleophilic exocyclic amino and hydroxyl functionalities and are highly charged at neutral pH. For these reasons, coupling paromomycin to solid support through a specific chemical group at low concentrations was desirable.

Rings I and II are common among the aminoglycosides (Figure 1c) and are in intimate contact with the RNA in the RNA−paromomycin structure (*13*). In contrast, rings III and IV of paromomycin are not common features of the aminoglycosides and do not make specific hydrogen bond contacts to the A-site RNA. For these reasons (and others explained below), ring IV was the target of our modification chemistry.

The 6‴-amino group of ring IV of paromomycin is the only amine attached to a nonbranched carbon and should be sterically more accessible and more nucleophilic than the other amino groups in the molecule. Previously, a report had shown that succinimidyl esters are preferentially attacked by the ϵ amino group of lysyl-tRNA rather than the α amino group under high pH buffer conditions (*18*) and that nucleophilicity of the ϵ amino group was reduced at lower pH. When both amines were fully deprotonated at high pH, the ϵ amine behaved as the better nucleophile. For similar reasons, we achieved selective linkage of NHS-activated compounds to the 6‴-amine of ring IV of paromomycin under high pH conditions. Conditions above pH = 10.0 were necessary to activate the 6‴-amine as a nucleophile.

Optimal column specificity and binding capacity were achieved by performing the coupling reactions such that the final concentration of paromomycin could not exceed 25 μM assuming 100% coupling efficiency. Higher levels of derivatization led to increased binding capacity at the expense of column specificity (see specificity discussions below). NHS esters are hydrolyzed at high pH, thus, columns prepared at pH = 10 while targeting the 6″-amine of ring IV most likely had lower final drug concentrations than those coupled at lower pH. Columns prepared identically at pH = 6.0 or 8.0 failed to bind A-site RNA with specificity. Low pH coupled matrix was equivalently effective in binding RNAs of unrelated sequence such as tRNA (see below).

Columns Derivatized with Paromomycin at High pH Are Linked through the 6‴-Amine of Ring IV. We determined that the position through which paromomycin covalently linked to the solid support was the 6‴-amine by performing a mock coupling reaction. The mock experiment coupled paromomycin to 6-(2,4-dinitrophenyl)aminohexanoic acid, succinimidyl ester (DNP−NHSE). We assume that the drug-dye coupling reaction mimics coupling of paromomycin to matrix because both reactions are mechanistically equivalent; DNP substitutes for the sepharose matrix in the mock experiment so that the reaction products can be analyzed by

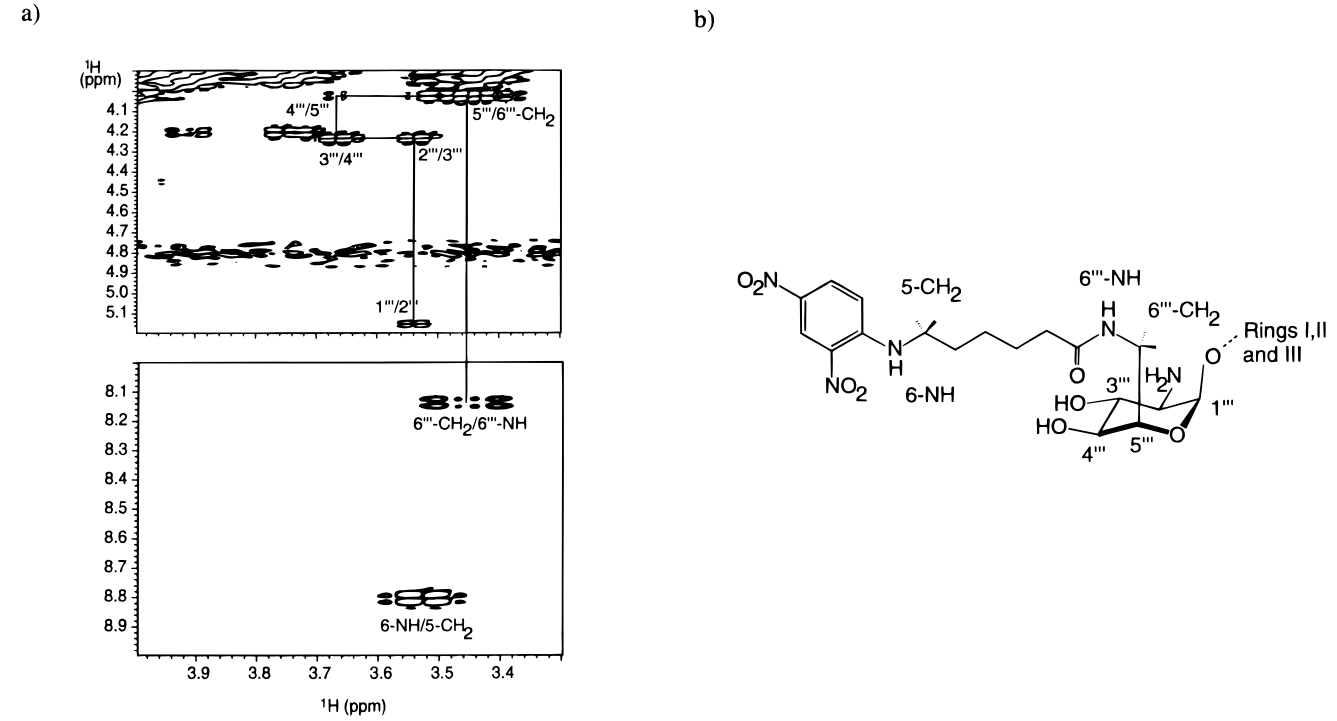

FIGURE 2: (a) Paromomycin conjugates to *N*-hydroxysuccinimide activated 6-(2,4-dinitrophenyl)aminohexanoic acid through the 6‴-amine of ring IV under the conditions of column matrix derivatization. The sugar proton region of the DQF−COSY spectrum in 99.99% D_2O correlates the ring IV spin system to the amide proton in the hexanoic acid linker (a separate experiment performed in 90% H_2O/10% H_2O); the diagrammed connectivity pathway illustrates that the 6‴-amine of paromomycin is linked to the carboxyl group of 6-(2,4-dinitrophenyl)amino hexanoic acid. (b) The chemical structure of 6-(2,4-dinitrophenyl)aminohexanoic acid linked to paromomycin is shown. Position numbers reflect those referenced in the DQF−COSY spectra.

standard techniques. DNP absorbs visible light (λ_{max} = 349 nm) and is bright yellow both in solution and as lyophilized powder; reactions of paromomycin with DNP−NHSE were easily monitored using TLC and HPLC.

Linkage of paromomycin to the DNP−NHSE reagent was performed in identical solution conditions as was done for coupling paromomycin to the column matrix. In addition, DNP−NHSE was coupled to paromomycin in solution at various pH. Electrospray mass spectrometry of crude reaction mixtures demonstrated that the drug-dye reaction products were monoacylated DNP−paromomycin compounds having a molecular weight of 896 amu. HPLC analysis indicated that the extent of reaction completion and the distribution of reaction products varied greatly with the pH of the reaction (data not shown). The major product for reactions carried out at pH = 10 comprised 58% of the reaction products (data not shown); the second most abundant product yield was 12.5%. The major reaction product at pH = 10 was linked through the 6‴-amine of ring IV; this was determined by double quantum filtered COSY (DQF−COSY) experiments performed on the HPLC-purified products. DQF−COSY spectra demonstrated that the resonance of the amide proton linking paromomycin to DNP was correlated to the proton resonances of ring IV (Figure 2). At lower pH coupling conditions, the 6‴-linked product was greatly diminished in favor of other species (data not shown).

Paromomycin Columns Coupled at pH 10 Are Specific for A-Site RNA. Several experiments demonstrated an increase in column specificity for A-site RNA when paromomycin was coupled to the matrix at pH = 10. First, A-site RNA was retained on the high pH derivatized matrix when loaded in the presence of a 5-fold molar excess of bulk tRNA (data not shown). This result suggests that linkage of paromomycin through the 6‴-position does not prevent the antibiotic from specifically binding to A-site RNA. Second, paromomycin-coupled column matrices had predictable RNA-binding behavior at various salt and pH conditions: binding of A-site RNA to the columns was reversible by raising the pH, the salt content of the buffer, or by addition of free paromomycin (data not shown). Third, columns with matrix coupled to spermine, glucosamine, or Tris base were unable to bind A-site RNA in buffer conditions where paromomycin-derivatized column matrix retained nearly 100% of the loaded RNA sample (Figure 3a). Finally, mutation of the A-site RNA sequence (G1491U and C1409U/G1491C), made to reflect paromomycin resistance mutations in ribosomal RNA, decreased binding to the paromomycin-coupled matrix (Figure 3b). These mutations in rRNA had previously been shown to give increased paromomycin resistance in vivo (*8*) and decreased paromomycin binding to the A-site RNA oligonucleotide in vitro (*5*).

The specificity of paromomycin-derivatized matrix for the wild-type A-site RNA sequence suggests that the tethered antibiotic retains its biologically relevant mode of binding. Direct footprinting of the DNP−paromomycin on the A-site RNA protected the same bases from chemical modification as seen for unmodified paromomycin, but the compound bound with approximately 10-fold reduced affinity (data not shown). In conclusion, the specificity of the column for binding A-site RNA was achieved by specifically coupling paromomycin to solid support at pH = 10 through the 6‴-amino position of ring IV at concentrations that could not exceed 25 μM. Using specifically derivatized matrix, we probed the A-site RNA for determinants that are required

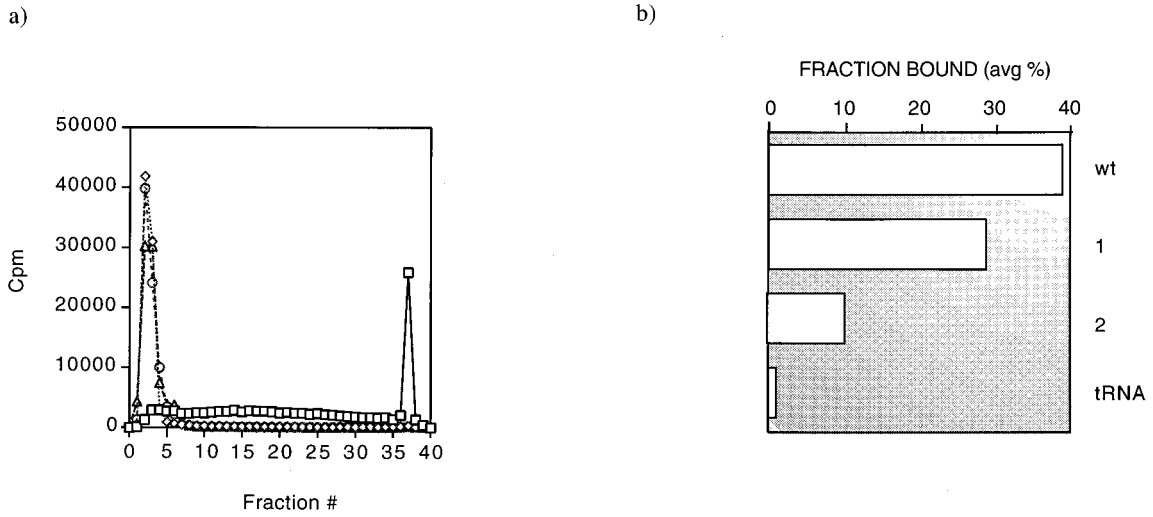

FIGURE 3: (a) Columns derivatized with cationic compounds such as spermine, glucosamine or Tris are unable to bind the A-site RNA under conditions where paromomycin-derivatized matrix retained nearly 100% of the loaded RNA. 3′ End-labeled RNA was loaded onto column matrix derivatized with various compounds at 4 °C using 10 mM Na_2PO_4, 80 mM NH_4OAc as running buffer at ~1 mL/min flow rate. (△) is the binding profile for matrix derivatized with Tris, (◇) spermine, (○) glucosamine, and (□) paromomycin. (b) Column matrix derivatized with paromomycin shows specificity for wild-type A-site RNA sequence. Paromomycin derivatized matrix binds A-site RNA (wt) while under the same experimental conditions (10 mM $NaH2PO_4$, 150 mM NH_4OAc running buffer, pH = 7.0, ~1 mL/min flow rate at 4 °C) where RNAs of unrelated nucleotide sequence like bulk tRNA are unable to bind. A-site RNA oligonucleotide mutants mimicking the A-site rRNA sequence of bacterial strains resistant to paromomycin have decreased binding affinity under the same assay conditions (see text). (1) A-site RNA containing G1491C/C1409U mutations, and (2) A-site RNA containing a G1491U mutation.

to interact with paromomycin.

Modification Interference Signal Is Sensitive to the Assay Conditions. Binding profiles of A-site RNA to the paromomycin column were identical in potassium or sodium cacodylate, Tris-HCl, and sodium phosphate buffers. Magnesium effects were tested at increments of 1 mM up to 20 mM. While RNA−drug interactions have previously been shown to be significantly magnesium dependent (*19*), A-site RNA binding to paromomycin-derivatized matrix was unaltered by increasing Mg^{2+} concentration in the running buffer other than decreasing binding affinity as would increasing ionic strength with monovalent salt. Binding curves observed for A-site RNA at various salt concentrations using NH_4Cl, KCl, and NaCl were superimposable. However, NH_4OAc buffers significantly shifted the binding curve toward higher affinity for reasons that we attribute to chaotropic salt effects. These salt effects also increase the apparent specificity of the derivatized matrix for A-site RNA (data not shown). Several steps in detecting the position of modifications are sensitive to buffer conditions. Therefore, thorough desalting of RNA samples is necessary for reliable comparison of RNAs from the flow-through and bound fractions. Use of NH_4OAc facilitated desalting because it could be removed by lyophilization after fractionation. In addition, samples were dialyzed against water following lyophilization.

Modification-interference experiments were run at salt and buffer conditions that gave a 50:50 ratio of flow-through to bound RNA using unmodified, end-labeled A-site RNA. These running conditions ensure that even slightly detrimental modifications to the RNA have large effects on the equilibrium population of the RNA−paromomycin complex. RNAs detrimentally modified selectively partition in the flow-through fractions, whereas unmodified RNA, or RNA containing a modification that is not disruptive to binding remain bound to the column. The best results for the phosphorothioate modification-interference experiments were obtained in conditions that gave a 60:40 ratio of flow-through to bound RNA using unmodified RNA.

Modifications That Disrupt Binding Are Centered around the Asymmetric Internal Loop Created by A1408, A1492, and A1493. Dilute amounts of modifying agent were used to modify RNAs to ensure that each RNA molecule had no more than one modification (*20*). Modification levels were established by quantitatively phosphorimaging modified and cleaved RNA separated on denaturing polyacrylamide gels to confirm that intact RNA constituted more than 90% of the total RNA. RNAs were thermally denatured during modification reactions to ensure that each susceptible position was equivalently accessible. RNA modifications were considered detrimental to paromomycin binding only if the position of modification was over-represented in the flow-through and under-represented in the bound fraction in comparison to the same sample of unfractionated, modified A-site RNA.

To probe backbone phosphate involvement in drug binding, ethylnitrosourea (ENU) was used to ethylate phosphate oxygens. Unfortunately, the phosphotriester that results from ENU modification is labile and backbone hydrolysis in the modified RNA occurred during the experiment obscuring the interference results. Thus, our assays using ENU could only be interpreted as testing the effect of backbone cleavage on paromomycin binding. Our conclusions from these experiments are that backbone cleavage anywhere in the internal loop of the A-site RNA disrupts binding (data not shown).

Specific drug-backbone contacts that contribute to complex stability were monitored by incorporation of phosphorothioate nucleotides into A-site RNA. In our hands, phosphorothioate linkages were significantly more stable than ENU induced phosphotriesters. Enzymatic incorporation of phosphorothioate NTPs replaces pro-*R* oxygen atoms with sulfur; the pro-*R* oxygen atom is oriented toward the major groove.

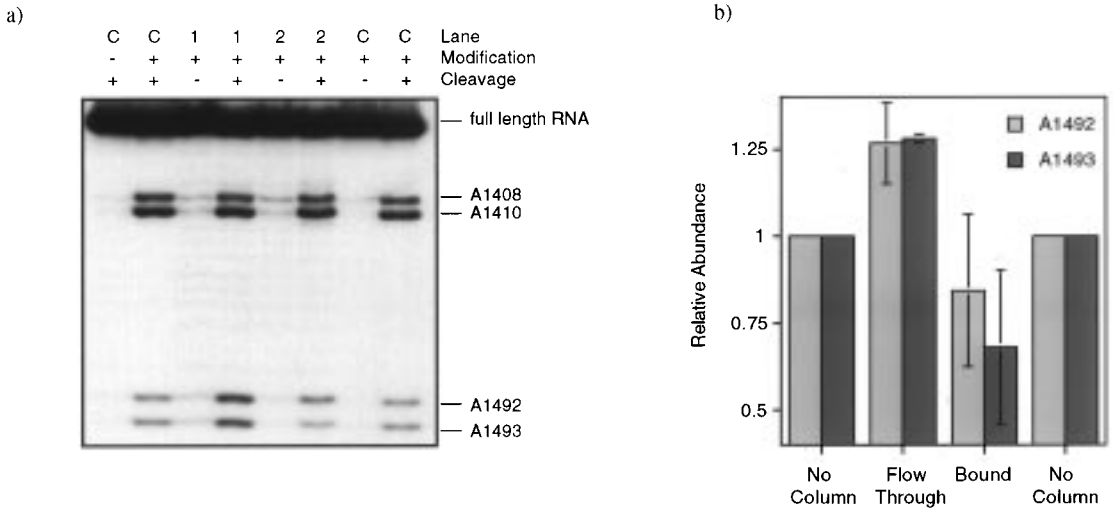

FIGURE 4: (a) Phosphorothioate nucleotides at A1492 and A1493 interfere with paromomycin binding. All lanes are run in duplicate to show that the RNA backbone is intact without induced cleavage. Lane 1 is the flow-through RNA fraction and lane 2 is the bound RNA fraction. For all figures, lane K is unmodified RNA and lane C is modified RNA that was not fractionated over the affinity column. (b) Quantitation of two phosphorothioate interference experiments demonstrates the importance of A1492 and A1493 phosphate oxygens to binding paromomycin-derivatized matrix. Normalized to modified RNA that was not fractionated over the paromomycin affinity column (C), RNAs with A1492 or A1493 phosphonyl sulfur modifications are over represented in the flow-through fraction and under represented in the bound fraction (corresponding to lanes 1 and 2 in Figure 4a, respectively).

Adenosine, guanosine, cytosine, and uridine phosphorothioate linkages were assayed independently. Quantitation illustrated that A-site RNA containing phosphonyl sulfur atoms at positions A1493 or A1492 selectively partitioned into the flow-through fractions indicative of interference with binding (Figure 4). Both A1492 and A1493 were on average more highly represented in the flow-through fraction (26 and 28%, respectively) and proportionally under-represented in the bound fraction (16 and 36%, respectively) with respect to RNA not partitioned by the column. On the bases of these data, A1493 phosphonyl oxygen modification had the most detrimental effect on binding (see discussion below). While the quantitation data presented in Figure 4 is only an average of two experiments, the significance of the interference statistics was supported by three additional experiments demonstrating the same pattern of interference. Detailed quantitative investigation of carboxyethylation and methylation-interference experiments was not necessary to establish significance of the data as the results were unambiguous.

Diethyl pyrocarbonate (DEPC) was used to monitor the importance of N7 positions of both adenosine and guanosine residues in the A-site RNA. Reaction of DEPC with purines results in the addition of a bulky carboxyethyl moiety and introduction of a positive charge at the N7 position (DEPC reacts ~10× more efficiently with adenine than guanine). Binding affinity of the A-site RNA to the derivatized column matrix was dramatically reduced upon carboxyethylation of A1493(N7) or A1408(N7). Binding affinity also was reduced for A1410(N7) modified RNA but to a lesser extent (Figure 5a). Longer film exposures indicated that carboxyethylation of G1494(N7), G1405(N7), or G1491(N7) was also detrimental to binding (data not shown). A1492(N7) carboxyethylation seems to enhance binding to paromomycin as RNA with this modification is under-represented in the flow-through fraction and over-represented in the bound fraction.

Dimethyl sulfate (DMS) methylates the N7 position of guanosine, the N1 position of adenosine, and the N3 position of cytosine. However, by standard direct strand scission methods, only modifications at the N7 of guanosine can be detected (*21*). Modification-interference experiments using DMS followed by direct strand scission confirmed the DEPC results in that methylation of G1494(N7) or G1491(N7) was significantly detrimental to binding. In addition, G1405-(N7) or G1497(N7) methylation had moderately detrimental effects on binding (Figure 5b).

To monitor modification at N1 and N3 positions in the RNA, an A-site RNA oligonucleotide was made with a 3′-overhang to which a primer was hybridized to enable primer extension (*22*). A-site RNA with this 3′-overhang had previously been shown to interact specifically with aminoglycoside antibiotics (*5*). Primer extension enabled us to determine that methylation of A1492(N1) and A1493(N1) greatly disrupted binding whereas A1408(N1) methylation had little effect on binding. This experiment also confirmed our previous data as to the importance of G1491(N7) and G1494(N7) for a high-affinity interaction with paromomycin (Figure 5c).

DISCUSSION

The modification-interference experiment is a sensitive monitor of the qualitative thermodynamic contribution of RNA−RNA and RNA−ligand contacts to complex stability. In contrast to mutagenesis or in vitro selection methods where entire bases are changed, only individual chemical groups are altered in the modification-interference experiment. The assay is extremely sensitive if carried out under conditions where the ligand−RNA complex is formed at 50% of saturation. Small thermodynamic perturbations (ca. 1 kcal/mol) to complex formation then lead to rather large changes in the relative populations of free and bound RNA.

A separation method for free and ligand-bound RNA is required to apply the modification-interference approach. The small size of aminoglycosides precludes the use of gel electrophoretic separation (gel mobility-shift); thus, we chose

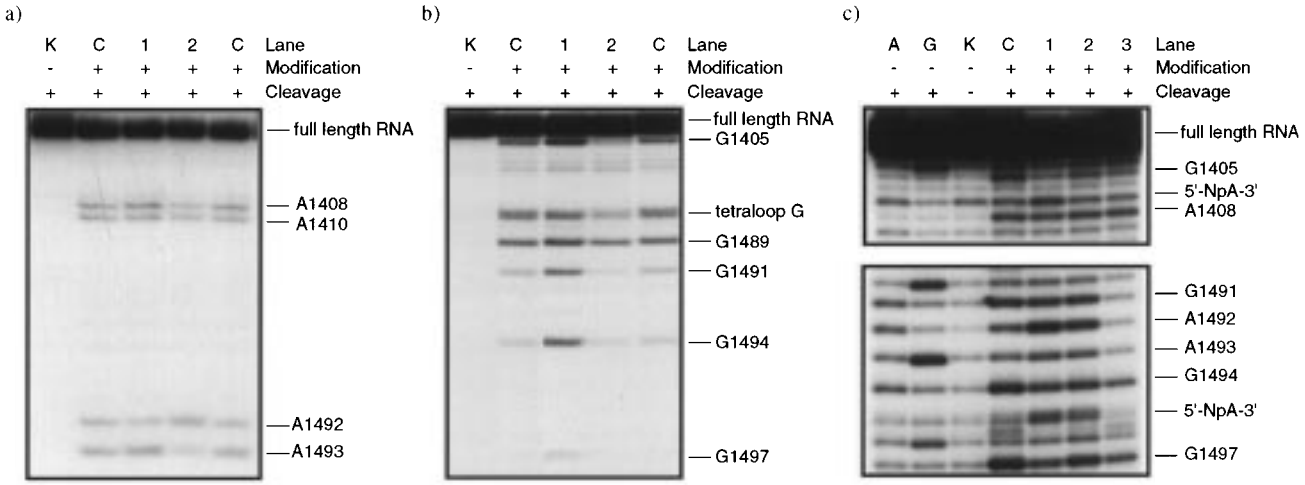

FIGURE 5: (a) Carboxyethylation of A1408(N7) or A1493(N7) gives strong interference to binding paromomycin derivatized matrix while A1410(N7) carboxyethylation gives weaker interference. Carboxyethylation of A1492(N7) appears to enhance binding. Lane 1 is the flow-through RNA fraction and lane 2 is the bound RNA fraction. (b) Methylation of G1491(N7) or G1494(N7) strongly interferes with paromomycin binding while G1405(N7) methylation gives weaker interference. In this experiment, lane 1 is the flow-through RNA fraction and lane 2 is the bound RNA fraction. (c) Primer extension of DMS modified A-site RNA with a 17 nucleotide 3′-overhang indicates that methylation of G1405(N7), G1491(N7), A1492(N1), A1493(N1) or G1494(N7) disrupts binding to paromomycin derivatized matrix. Lanes A and G are adenine and guanine sequencing lanes, respectively. Lane 1 is the flow-through RNA fraction and lane 2 is the bound RNA fraction. 5′-NpA-3′ indicates points of nonspecific hydrolysis in the RNA backbone.

a liquid chromatographic method. Commercial column matrices are available for aqueous *N*-hydroxysuccinimide-activated ester coupling to amines. Success using the affinity columns was dependent upon coupling the drug to a nonessential portion of the aminoglycoside at low enough drug concentration to avoid nonspecific RNA binding to the derivatized matrix due to high-density cationic charge. Matrix highly derivatized with aminoglycosides resulted in an electrostatic contribution to binding that predominated over sequence-specific RNA binding.

Solution studies of the RNA−paromomycin complex suggested that the 6‴-amine of paromomycin was the best site of covalent attachment to column matrix. Because the 6‴-amine is the only amino group in paromomycin attached to a nonbranched carbon, it could be specifically targeted under the proper conditions. HPLC, mass spectrometry, and NMR were used to characterize the conjugate formed in a reaction between paromomycin and DNP, a compound that mimics the column resin used in the modification-interference experiments. These experiments support our contention that paromomycin was selectively coupled to the column resin through the desired 6‴-amine position at high pH.

Modification of chemical groups in the major groove of the A-site RNA within the asymmetric internal loop strongly interferes with binding to paromomycin (Figure 6). The subset of chemical groups within the A-site RNA that were required for binding was determined by quantitating the partition of modified RNA molecules toward either the flow-through or bound populations upon fractionation over the paromomycin affinity column. An RNA modification was interpreted as being detrimental to paromomycin binding only if the position of modification was over-represented in the flow-through and under-represented in the bound fractions.

By these criteria, two important hydrogen-bonding contacts between paromomycin and the RNA backbone have been identified through phosphorothioate modification-interference experiments. Replacement of the nonbridging, major groove phosphonyl oxygen by sulfur at positions A1492 and A1493

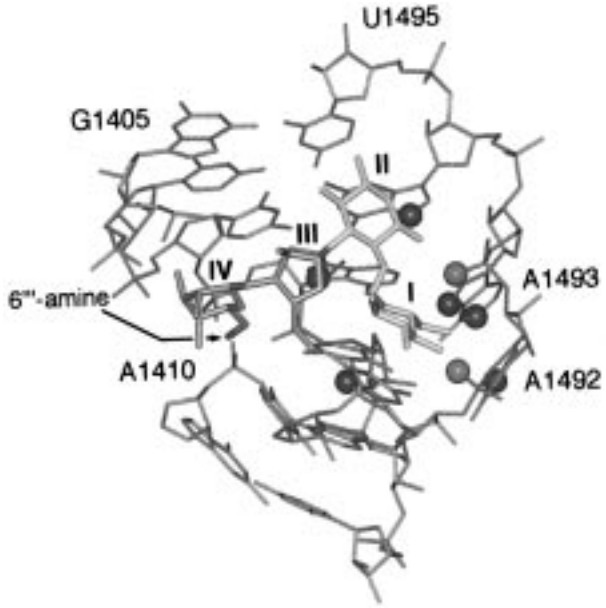

FIGURE 6: The subset of chemical groups within A-site RNA that give strong modification interference to drug binding are clustered around the paromomycin binding pocket (*5*, *8*). The RNA is illustrated in gray and paromomycin rings III and IV are in purple and rings I and II in yellow. Positions that give strong interference to paromomycin binding are modeled as spheres into the NMR structure. RNA modifications that are strongly deleterious to paromomycin are within the asymmetric internal loop formed by the bulged adenosine and the A1408-A1493 base pair. Nitrogen groups critical to binding are shown in blue, phosphate oxygens in red. The 6‴-amine of ring IV of paromomycin is shown in green.

specifically disrupts hydrogen bonds with the drug or distorts a specific backbone geometry that is required for binding. Phosphorothioate-interference data is usually limited to those phosphates that are of great importance to structure or function of RNA molecules because little steric or electrostatic penalty is introduced by these modifications. On the basis of quantitation of the interference results, A1493 phosphate appears to be of greater importance to drug binding

than A1492 phosphate (Figure 4).

Both A1492 and A1493 phosphate oxygens are in close proximity to ring I of paromomycin in the reported drug−RNA NMR structure and could make direct contact with 3′, 4′, and/or 6′ hydroxyl groups of the drug, positions that are correlated with drug activity (*23*). Organisms that harbor enzymes that modify the aminoglycosides at any of these positions are resistant to paromomycin (*24*). Also, A1492 and A1493 phosphate torsion angles are dramatically distorted upon drug binding (*11*). Thus, based on the structural and modification-interference data, distortion of the backbone at A1492/93 and/or specific drug contacts with phosphate oxygens at these positions must be central to complex formation.

Methylation of G1494(N7) yields the strongest drug-binding interference using DMS as detected by direct strand scission. Modification at this position must produce a strong thermodynamic penalty to binding. In the paromomycin−RNA complex, G1494(N7) interacts directly with the 3-amino group of ring II of paromomycin, a common component of all aminoglycoside antibiotics. Consistent with these data, previous in vitro results have shown that mutation of C1407-G1494 base pair to G1407-C1494 is strongly deleterious to paromomycin binding (*5*).

Methylation of G1491(N7) also interferes with paromomycin binding. This base, while not in direct hydrogen bond contact to the drug in the NMR structure, is in close proximity to ring III of the antibiotic and has previously been genetically linked to paromomycin resistance in vivo (*25*). Methylation of G1491(N7) probably leads to significant steric and electrostatic penalties to binding.

Methylation of G1405(N7) and G1497(N7) give weak drug-binding interference correlating with their increased distance from the drug-binding pocket. The most likely explanation for interference is that methylation increases positive charge density in the major groove close to the drug-binding site, which reduces electrostatic contributions of paromomycin-binding affinity. Consistent with our modification-interference observations, bacterial enzymes that methylate the A-site of rRNA at position G1405(N7) do not confer resistance to paromomycin or any of the neomycin class antibiotics; these enzymes impart resistance to gentamicin and kanamycin, which are in a distinct structural class of aminoglycoside antibiotics (*3*, *26*).

Data regarding carboxyethylation and methylation of adenosines in the A-site RNA highlights the importance of the A1408-A1493 base pair and the conformation of A1492 underscoring the role of RNA−RNA interactions required for complex formation. NMR studies show that upon RNA−drug complex formation, the dynamic processes of A1493 become greatly reduced, A1492 stacks beneath A1493 and A1493(N7) moves within hydrogen-bonding distance of A1408(N1) (*11*). The specific geometry of the A1408-A1493 base pair is essential to formation of the proper drug-binding pocket as antibiotic binding is greatly diminished by mutation of either A1408 or A1493 to other bases (*5*). Consistent with the structural and mutagenesis data, carboxyethylation of A1493(N7) or A1408(N7) by DEPC strongly interferes with paromomycin binding.

Previous results suggest that the nucleotide identity at position A1492 is not critical for binding (*5*). However, involvement of A1492 in the antibiotic-binding pocket is unequivocal. Whereas mutation of A1492 to guanidine or cytidine has a small detrimental effect on paromomycin binding in vitro, its deletion abolishes binding (*5*). Consistent with the mutagenesis data, DEPC modification of A1492-(N7) has no energetic penalty on binding. However, several modification-interference data suggest a specific role for the conformation of A1492 in forming the antibiotic-binding pocket. First, carboxyethylation of A1492(N7) enhances binding to paromomycin; RNAs modified at this position are over-represented in the bound population of RNA and under-represented in the flow-though RNA pool (see lane 2, Figure 5a). On the basis of the structure, A1492(N7) is positioned in the minor groove such that carboxyethylation at the N7 position should not result in steric interference to paromomycin binding. Introduction of a hydrophobic group at A1492(N7) may contribute to an important hydrophobic interaction that occurs in the complex, such as stacking of ring I of paromomycin on G1491. Alternatively, the positive charge at the N7 position of A1492 may stabilize the local phosphate distortion induced by drug-binding. Further experiments are required to resolve such issues.

The second piece of data suggesting that the conformation of A1492 in the binding pocket is important to drug-binding is that modification of A1492(N1) strongly interferes with binding. By reverse transcription, we determined that A1492(N1) methylation is greatly disruptive to binding. In addition, A1493(N1) methylation is greatly disruptive to binding. As will be discussed in a later section, A1408-(N1) methylation does not significantly reduce binding affinity.

Several lines of reasoning could explain the A1492(N1) and A1493(N1) binding interference data. Methylation of A1492(N1) or A1493(N1) may disrupt base stacking. Base modifications are known to dramatically alter base-stacking geometry (*27*). However, it is also reasonable to suggest that hydrogen bonds are formed at these positions that are important to complex stability. A1492 is not well-defined by the NMR data (*8*), but in the majority of structures, A1492(N1) is within hydrogen-bonding distance of nearby hydrogen bond donor groups in the minor groove of the RNA. On the basis of the existing evidence, we cannot rule out the possibility that A1492(N1) and A1493(N1) make important direct or water-mediated RNA−RNA contacts required for the formation of the drug-binding pocket. Since carboxyethylation of A1492 also effects binding, it is likely that the conformation of A1492 greatly influences the overall structure in this region of A-site RNA.

Although A1408(N1) is in close proximity to the paromomycin-binding site as seen in the NMR structure and involved in the formation of an A1408-A1493 base pair, bacterial enzymes that methylate the A-site of rRNA at position A1408(N1) confer resistance to kanamycin, apramycin, neamine, and ribostamycin, but only a slight resistance to neomycin or paromomycin (*28*). This in vivo observation is consistent with our modification-interference data which suggests that contacts made by A1408(N1) only weakly contribute to paromomycin binding.

The most striking modification-interference data obtained from our experiments are from A1492(N1), A1493(N1), and G1494(N7) methylation. A1492(N1) and A1493(N1) positions, which are not oriented such that they can make direct contact with paromomycin, give as strong of a modification-

interference signal as G1494(N7), which makes direct hydrogen bond contact with the drug. The fact that these three positions give roughly equivalent binding interference when methylated suggests that the thermodynamic consequences of disrupting indirect RNA−RNA contacts are as deleterious as disrupting a direct RNA−paromomycin interaction. Strikingly, bacterial methylases modify A1408(N1) and G1405(N7) but not A1492, A1493, or G1494, the nucleotides that are most important to paromomycin binding. These data further suggest that these positions in rRNA are essential to ribosome function.

Modification-interference experiments based on affinity chromatography have allowed us to determine which residues of the A-site RNA contribute to paromomycin binding. Coupling paromomycin to solid support through the 6‴-amine of ring IV was crucial to A-site specific RNA binding and modification-interference signal. Our results underscore the role of RNA−RNA and RNA−paromomycin contacts to the RNA−drug interaction. These data are consistent with the NMR structure of the drug−RNA complex and contribute to an understanding of aminoglycoside binding, resistance mechanisms, and antibiotic function. These data should enable us to perform more detailed NMR investigations of the A-site RNA structure with specific RNA modifications to determine the effects on RNA structure and aminoglycoside binding.

ACKNOWLEDGMENT

The authors would like to thank Eric Lau, Prof. H. Noller, Rachel Green, and Simpson Joseph for support and critical discussion.

REFERENCES

1. Moazed, D., and Noller, H. F. (1987) *Nature 327*, 389−394.
2. Paci, M., Pon, C., and Gualerzi, C. (1983) *EMBO J. 2*, 521−526.
3. Piendl, W., Böck, A., and Cundliffe, E. (1984) *Mol. Gen. Genet. 197*, 24−29.
4. Bilgin, N., Richter, A. A., Ehrenberg, M., Dahlberg, A. E., and Kurland, C. G. (1990) *EMBO J. 9*, 735−739.
5. Recht, M. I., Fourmy, D., Blanchard, S. C., Dahlquist, K. D., and Puglisi, J. D. (1996) *J. Mol. Biol. 262*, 421−436.
6. Purohit, P., and Stern, S. (1994) *Nature 370*, 659−662.
7. Miyaguchi, H., Narita, Hidehiko, Sakamoto, K., and Yokoyama, S. (1996) *Nucleic Acids Res. 24*, 3700−3706.
8. Fourmy, D., Recht, M. I., Blanchard, S. C., and Puglisi, J. D. (1996) *Science 274*, 1367−1371.
9. DeStasio, E. A., Moazed, D., Noller, H., and Dahlberg, A. E. (1989) *EMBO J. 8*, 1213−1216.
10. Moazed, D., and Noller, H. F. (1986) *Cell 47*, 985−994.
11. Fourmy, D., Yoshizawa S., and Puglisi, J. D. (1998) *J. Mol. Biol. 277*, 333−345.
12. Powers, T., and Noller, H. F. (1994) *J. Mol. Biol. 235*, 156−172.
13. Fourmy, D., Recht, M. I., and Puglisi, J. D. (1998) *J. Mol. Biol. 277*, 347−362.
14. Wyatt, J. R., Chastain, M., and Tinoco, I. J. (1991) *BioTechniques 11*, 764−769.
15. Ruffner, D. E., and Uhlenbeck, O. C. (1990) *Nucleic Acids Res. 18*, 6025−6029.
16. Peattie, D. A., and Herr, W. (1981) *Proc. Natl Acad. Sci. U.S.A. 78*, 2273−2277.
17. Rudinger, J., Puglisi, J. D., Pütz, J., Schatz, D., Eckstein, F., Florentz, C., and Giegé, R. (1992) *Proc. Natl. Acad. Sci. U.S.A. 89*, 5882−5886.
18. Vlassov, V. V., Giege, R., and Ebel, J.-P. (1981) *Eur. J. Biochem. 119*, 51−59.
19. Famulok, M., and Hüttenhofer, A. (1996) *Biochemistry 35*, 4265−4270.
20. Puglisi, J. D., Wyatt, J. R., and I. Tinoco, J. (1991) *Acc. Chem. Res. 24*, 152−158.
21. Peattie, D. A., and Gilbert, W. (1980) *Proc. Natl. Acad. Sci. U.S.A. 77*, 4679−4682.
22. Moazed, D., Stern, S., and Noller, H. F. (1986) *J. Mol. Biol. 187*, 399−416.
23. Benveniste, R., and Davies, J. (1973) *Antimicrob. Agents Chemother. 4*, 402−409.
24. Shaw, K. J., Rather, P. N., Hare, R. S., and Miller, G. H. (1993) *Microbiol. Rev. 57*, 138−163.
25. DeStasio, E. A., and Dahlberg, A. E. (1990) *J. Mol. Biol. 212*, 127−133.
26. Beauclerk, A. A., and Cundliffe, E. (1987) *J. Mol. Biol. 193*, 661−671.
27. Cundliffe, E. (1990) Recognition Sites for Antibiotics within rRNA. in *The Ribosome Structure, Function and Evolution* (Hill, W. E., Dahlberg, A., Garrett, R. A., et al., Eds.) pp 479−490, Washington, DC, American Society for Microbiology.
28. Bugg, C. E., and Thewalt, U. (1969) *Biochem. Biophys. Res. Commun. 37*, 623−629.
29. Botto, R. E., and Coxon, B. (1983) *J. Am. Chem. Soc. 105*, 1021−1028.

BI973125Y